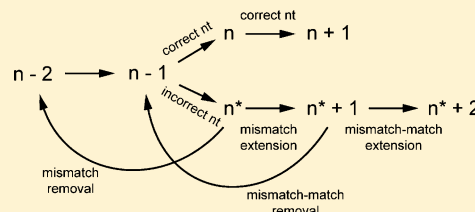


# Fidelity of RNA Polymerase II Transcription: Role of Rpb9 in Error Detection and Proofreading

Kevin Knippa and David O. Peterson\*

Department of Biochemistry and Biophysics, Texas A&M University, College Station, Texas 77843-2128, United States

**ABSTRACT:** The role of the small RNA polymerase II subunit Rpb9 in transcriptional proofreading was assessed in vitro. Transcription elongation complexes in which the 3' end of the RNA is not complementary to the DNA template have a dramatically reduced rate of elongation, which provides a fidelity checkpoint at which the error can be removed. The efficiency of such proofreading depends on competing rates of error propagation (extending the RNA chain without removing the error) and error excision, a process that is facilitated by TFIIS. In the absence of Rpb9, the rate of error propagation is increased by 2- to 3-fold in numerous sequence contexts, compromising the efficiency of proofreading. In addition, the rate and extent of TFIIS-mediated error excision is also significantly compromised in the absence of Rpb9. In at least some sequence contexts, Rpb9 appears to enhance TFIIS-mediated error excision by facilitating efficient formation of a conformation necessary for RNA cleavage. If a transcription error is propagated by addition of a nucleotide to the mismatched 3' end, then the rate of further elongation increases but remains much slower than that of a complex with a fully base-paired RNA, which provides a second potential fidelity checkpoint. The absence of Rpb9 also affects both error propagation and TFIIS-mediated error excision at this potential checkpoint in a manner that compromises transcriptional fidelity. In contrast, no effects of Rpb9 on NTP selectivity were observed.



The accuracy of transcription is of clear importance in gene expression, as errors in transcription can result in proteins with altered function. The error frequency of eukaryotic RNA polymerase II (pol II) in vitro has been measured in a number of studies,<sup>1,2</sup> and estimates vary between about  $10^{-3}$  and  $10^{-5}$  errors per nucleotide incorporated, depending on the template and the concentration and type of divalent metal ion present. Recent studies have suggested one mechanism by which pol II (as well as other multisubunit RNA polymerases) discriminate correct, template-specified nucleoside triphosphates (NTPs) from incorrect NTPs and dNTPs. This selectivity depends on the trigger loop, a mobile structural element within Rpb1, the largest of the pol II subunits. The trigger loop can move into proximity of the active site, a conformational change that serves to trap the correct NTP and position functional groups required for catalysis.<sup>3–5</sup> The role of the trigger loop in transcription has been thoroughly discussed in several recent reviews.<sup>6–9</sup>

In addition to substrate selectivity, transcriptional fidelity can also depend on proofreading in which mistakes can be excised from the growing transcript as it is synthesized. Pol II possesses an intrinsic nuclease activity that cleaves single nucleotides or short oligonucleotides from the 3' ends of nascent RNAs, and this activity can be enhanced by the accessory protein TFIIS (for a review, see ref 10). Crystal structures of pol II-TFIIS complexes have revealed that a C-terminal zinc ribbon domain of TFIIS inserts into the active site of the polymerase where the side chains of two acidic residues (TFIIS D290 and E291 in *Saccharomyces cerevisiae*) coordinate a metal and position a water molecule for hydrolysis.<sup>11,12</sup> Deletion of *DST1*, the gene that encodes yeast TFIIS, has very little measurable effect in

some in vivo assays designed to assess fidelity,<sup>13,14</sup> but easily detectable effects have been seen in others.<sup>15</sup> These differences may reflect differential sensitivities of the assays or, perhaps, that the indirect readout these assays provide is, at least in some cases, more sensitive to parameters other than transcriptional fidelity. It is clear, however, that intrinsic and TFIIS-mediated cleavage activities are important in vivo. TFIIS with alanine substitutions at D290 and E291 not only lacks the ability to stimulate cleavage but also inhibits intrinsic cleavage activity in vitro and, when overexpressed, confers a severe growth defect when it is the only TFIIS present in yeast.<sup>16</sup> TFIIS, as well as its bacterial counterpart GreA, can stimulate removal of misincorporated NTPs in vitro, consistent with a possible role in proofreading.<sup>2,17,18</sup>

Rpb9 is a small (122 amino acids in *S. cerevisiae*) pol II subunit that is highly conserved among eukaryotes.<sup>19,20</sup> Although Rpb9 is not essential for growth in yeast, *rpb9*-null mutants have growth and drug-hypersensitivity phenotypes<sup>21–23</sup> as well as upstream shifts in transcription start sites for a number of genes.<sup>24–26</sup>

Several studies have suggested a role for Rpb9 in transcriptional fidelity. Deletion of *RPB9* was shown to increase expression of functional Can1 protein arising from a nonsense allele of *CAN1*, presumably because of transcription errors, and sequence analysis of cDNAs derived from a *rpb9Δ* strain provided direct evidence of increased base substitutions and insertions.<sup>13</sup> Increased expression of a functional protein from a

Received: July 17, 2013

Revised: October 1, 2013

Published: October 8, 2013



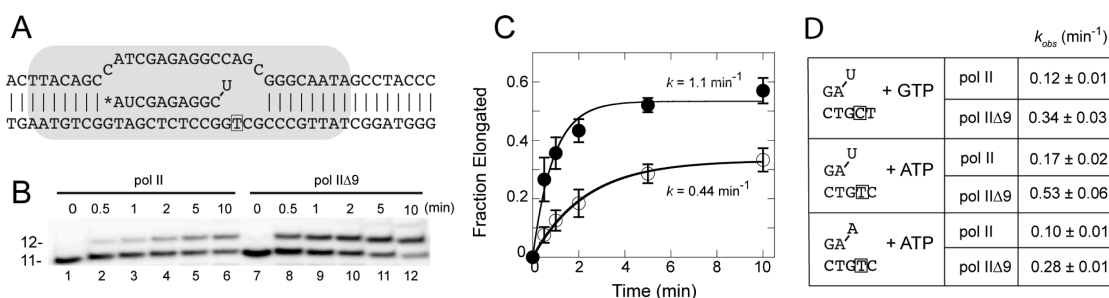


**Figure 1.** Effect of Rpb9 on extension of a mismatched 3' end. (A) Schematic representation of an assembled elongation complex. Template and nontemplate DNA oligos depict the transcription bubble.  $^{32}\text{P}$ -labeled RNA with a 3' mismatch is between the DNA strands. The small box indicates the template position for extension by the next correct NTP, and the shaded area represents the approximate region associated with pol II. (B) Time course of 3'-mismatch extension. The EC depicted in panel A was assembled with purified pol II (lanes 1–6) or pol IIΔ9 (lanes 7–12) and incubated with ATP (250  $\mu\text{M}$ ). Aliquots were removed at the indicated times, and the products were separated by denaturing polyacrylamide gel electrophoresis and visualized on a phosphorimager. (C) Quantitation of the extension time course. The fraction of ECs extended to 12 nt was plotted versus time and fit to a single exponential equation (open circles, pol II; closed circles, pol IIΔ9). Error bars indicate the SD for three independent experiments. (D) Summary of 3'-mismatch extension rates for different sequence contexts. Rates of mismatch extension were determined with ECs that differed from that shown in panel A as depicted (with complementary template and nontemplate strands). The rate constants for extension with the next correct NTP (250  $\mu\text{M}$ ) were calculated for pol II and pol IIΔ9. Errors indicate the chi-square value for the fit of the exponential curve to the averages of individual time points.

plasmid-borne nonsense allele of *Escherichia coli lacZ* in *rpb9Δ* yeast has also been observed.<sup>27</sup> In addition, it has been reported that, in at least one sequence context, the absence of Rpb9 affects substrate selectivity in vitro, decreasing the ability of the polymerase to discriminate between correct and incorrect NTPs.<sup>28</sup>

Indirect evidence suggests that Rpb9 may affect transcriptional proofreading. The Rpb9 homologues in RNA polymerases I and III (A12.2 and C11, respectively) are required for the intrinsic nuclease activity of these polymerases,<sup>29–31</sup> which are much more robust than that of pol II, and the related archaeal protein TFS has been shown to affect transcriptional fidelity in vitro.<sup>32</sup> All of these proteins contain highly related N-terminal and C-terminal zinc ribbon domains characterized by the zinc chelating motif (CX<sub>2</sub>CX<sub>n</sub>CX<sub>2</sub>C).<sup>31–34</sup> Moreover, a chimeric protein in which the C-terminal 35 amino acids of Rpb9 are replaced by the 25 C-terminal residues of C11 dramatically increases the intrinsic nuclease activity of pol II.<sup>35</sup> Other in vitro experiments indicate that pol II lacking Rpb9 (pol IIΔ9) is less responsive to TFIIS-mediated transcript cleavage at defined pause and arrest sites,<sup>2,36</sup> but a potential effect of Rpb9 on cleavage of mismatched 3' ends generated by transcription errors has not been explored.

The present study directly examines potential roles of Rpb9 in transcriptional proofreading in vitro. We show that Rpb9 is important in slowing pol II elongation after a misincorporation event in order to provide a checkpoint during which proofreading can occur. We have identified two such checkpoints, one immediately after the incorrect NTP has been incorporated and a second located one nucleotide downstream of the misincorporation. In addition, in at least some sequence contexts, Rpb9 is required for a pol II elongation complex (EC) containing an error at its 3' end, or immediately adjacent to its 3' end, to adopt efficiently a conformation in which TFIIS-mediated cleavage can occur. In addition and in contrast to a previous report,<sup>28</sup> we show that in at least two sequence contexts the effect of Rpb9 on selectivity is minimal, suggesting that its role in proofreading, which we observed in a wide variety of sequence contexts, may be the dominant effect of Rpb9 on fidelity.

## EXPERIMENTAL PROCEDURES

### Yeast Strains and Preparation of Whole Cell Extract.

The parental *S. cerevisiae* strain was derived from a protease-deficient BJ5464 strain in which the *RPB3* ORF had been modified to contain two affinity tags, a 6×-His tag and a 26 amino acid sequence recognized by BirA, a bacterial biotin protein ligase.<sup>37</sup> This parental strain was generously provided by Mikhail Kashlev. The *RPB9* ORF was deleted from this strain (*rpb9Δ::kanMX4*) by PCR-mediated one-step gene disruption.<sup>38,39</sup> Whole cell extract (WCE) was prepared as described by Kireeva et al.<sup>37</sup>

**Pol II and TFIIS Purification.** Pol II and pol IIΔ9 were purified essentially as described by Kireeva et al.<sup>37</sup> with modifications described by Sydow et al.<sup>40</sup> The recombinant TFIIS used in assays with purified pol II was a cleavage-competent N-terminal truncation of TFIIS (TFIIS Δ2–146)<sup>3</sup> and was generously provided by Craig Kaplan.

**RNA Labeling and RNA–DNA Hybrid Formation.** RNA oligos (16.7 pmol) were labeled with an equimolar amount of [ $\gamma$ - $^{32}\text{P}$ ]ATP (3000 Ci/mmol) using T4 polynucleotide kinase in transcription buffer TB(40) [20 mM Tris-HCl (pH 7.9), 40 mM KCl, 5 mM MgCl<sub>2</sub>, and 2 mM 2-mercaptoethanol]. It was then annealed with the appropriate DNA template strand (16.7 pmol) as described by Kireeva et al.<sup>37</sup> Unlabeled NTPs were from GE Healthcare.

**Elongation Complex Assembly and in Vitro Transcription.** The assembly of elongation complexes (ECs) was essentially as described by Kireeva et al.<sup>37</sup> Purified pol II or pol IIΔ9 (250 ng) or WCE (25  $\mu\text{L}$ ) was added to 25  $\mu\text{L}$  of Ni<sup>2+</sup>-NTA beads (Qiagen) that had been washed with TB(40). Binding and wash steps were performed at room temperature using an orbital shaker at 1000 rpm. After 30 min, the beads were washed with 1 mL of TB(1000) (same composition as TB(40) except with 1 M KCl) for 10 min and then washed three times with 1 mL of TB(40). RNA–DNA hybrid (1 pmol) was then incubated with the beads for 10 min in a total volume of 100–150  $\mu\text{L}$  followed by addition of the nontemplate DNA strand (10 pmol) for an additional 10 min. ECs were then washed with 1 mL of TB(1000) for 10 min and then three times with 1 mL of TB(40). The final suspension of immobilized ECs was in 100–200  $\mu\text{L}$  of TB(40). After

addition of NTPs or TFIIS, aliquots (10  $\mu$ L) were removed at various times and added to a tube containing 10  $\mu$ L of 2 $\times$  gel loading buffer [10 M urea, 50 mM EDTA (pH 7.9), 0.005% bromophenol blue, and 0.005% xylene cyanol]. Products were separated by polyacrylamide gel electrophoresis with a gel containing 20% acrylamide (19:1 acrylamide/bisacrylamide), 7 M urea, and TBE [50 mM Tris-borate (pH 8.3), 1 mM EDTA]. ECs with mismatched RNAs using WCE were assembled as above except that the 10 min wash times were shortened to 1 min to reduce the extent of cleavage during assembly. RNAs were visualized and quantitated with a Phosphorimager (Bio-Rad PharosFX Plus). Least-squares curve fits and the determination of the errors associated with the fits were performed with Kaleidagraph software (Synergy Software).

## RESULTS

**Absence of Rpb9 Increases the Rate of Elongation beyond a Mismatched 3' End.** Transcriptional proofreading involves competing rates of error propagation and error elimination. To explore the potential effect of Rbp9 on error propagation, we immobilized purified pol II or pol II  $\Delta$ 9 with Ni<sup>2+</sup>-NTA beads via a 6 $\times$ -His tag on Rpb3, and ECs were assembled with DNA and RNA oligonucleotides<sup>37</sup> in which the 11 nt RNA was 5'-end labeled with <sup>32</sup>P (Figure 1A).

Using an EC with a G–U mismatch at its 3' end to mimic a transcription error, we followed the time-course of extension with ATP (the next correct nucleotide) (Figure 1B). The fraction extended to 12 nt was plotted against time, and the data were fit to a single exponential equation (Figure 1C). The rate of mismatch extension for pol II  $\Delta$ 9 ( $k_{\text{obs}} = 1.1 \text{ min}^{-1}$ ) was 2 to 3 times faster than for pol II ( $k_{\text{obs}} = 0.44 \text{ min}^{-1}$ ). Assays with higher concentrations of ATP, up to 1 mM, gave essentially identical results, strongly suggesting that the ATP concentration used here (250  $\mu$ M) is near saturating in this assay (data not shown). Interestingly, the number of complexes capable of being extended, which is generally 80–95% in assays in which the template and nascent RNA are completely complementary (for an example, see Figure 7), was significantly lower with these mismatched ECs; only about 30% of the pol II and 50% of the pol II  $\Delta$ 9 complexes were extended at the reaction end points.

To explore mismatch extension in other sequence contexts, we assembled ECs in which the next correct NTP was changed from ATP to GTP or in which either the penultimate or the mismatched ribonucleotide was altered. Each of the sequence changes had an effect on the absolute rate of mismatch extension, but in every context, pol II  $\Delta$ 9 was faster by 2–3-fold (Figure 1D). Among the sequence contexts tested, the fastest rate observed was with an EC containing a G–C base pair just preceding a G–U mismatch. Extension rates determined by rapid-quench kinetics using comparable ECs with completely matched RNAs have been reported to be 1000-fold or more higher than the rates we have determined with 3'-end-mismatched ECs.<sup>28</sup> Thus, a slow rate of mismatch extension provides a significant checkpoint that could be exploited for proofreading, as was first described by Thomas et al.<sup>18</sup> The fraction of complexes that was subject to extension also varied in each of these sequence contexts, but, in contrast to the sequence context represented in Figure 1A, the fraction of ECs that could be elongated in each of the other contexts was not significantly different for pol II and pol II  $\Delta$ 9. This difference may depend on the G–C base pair immediately preceding the

mismatch, as it is present only in the sequence context shown in Figure 1A.

**Rpb9 Promotes TFIIS-Mediated Cleavage of Transcripts with a Mismatched 3' End.** The observed increase in the rate of error propagation in the absence of Rpb9 is relevant for fidelity only if it is not offset by a corresponding increase in the rate of error elimination. As has been observed in several studies,<sup>3,35,36</sup> we have not detected significant endogenous cleavage activity with pol II ECs at near-neutral pH. However, when ECs with mismatched 3' ends were incubated in the presence of a cleavage-competent<sup>41</sup> N-terminal truncation of TFIIS (TFIIS $\Delta$ 2–146<sup>3</sup>), relatively slow ( $k_{\text{obs}} = 0.05 \text{ min}^{-1}$ ) but efficient (65% cleavable) cleavage was apparent (Figure 2

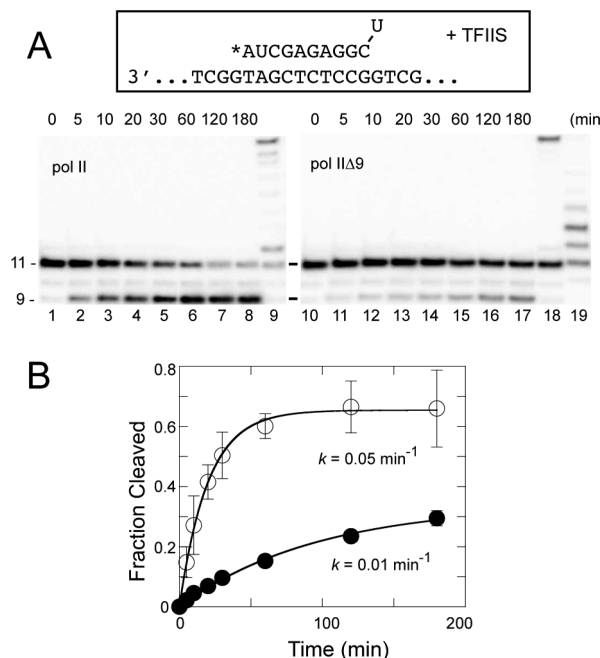


**Figure 2.** Effect of Rpb9 on TFIIS-mediated cleavage of a 3'-mismatched end. (A) Time course of cleavage. ECs with a mismatched 3' end identical to that shown in Figure 1A were assembled with purified pol II (lanes 1–9) or pol II  $\Delta$ 9 (lanes 10–19). An abbreviated depiction of the EC is shown here for reference. These ECs were incubated with purified recombinant TFIIS (10  $\mu$ M). Aliquots were removed at the indicated times, and the products were separated by denaturing polyacrylamide gel electrophoresis and visualized on a phosphorimager. After 180 min, ATP, CTP, and GTP (10  $\mu$ M each) were added to the reaction and incubated for 30 s (lanes 9 and 18). An aliquot of the pol II  $\Delta$ 9 ECs was incubated for 60 min with ATP (250  $\mu$ M) (lane 19). (C) Quantitation of the cleavage time course. The fraction of ECs cleaved to 9 nt was plotted against time and fit to a single exponential equation (open circles, pol II; closed circles, pol II  $\Delta$ 9). Error bars indicate the SD for three independent experiments.

panel A, lanes 1–8, and panel B, open circles). Furthermore, the observed removal of 2 nt from the RNA was as expected for a TFIIS-mediated process.<sup>42</sup> The cleaved RNAs remained in active ECs, as addition of ATP, CTP, and GTP (10  $\mu$ M each) after 180 min resulted in rapid extension of the cleavage-generated 9-mer to longer products up to 20 nt, whereas the relatively small amount of 11-mer remaining (still containing the mismatch) was not efficiently extended during the 30 s incubation with NTPs (Figure 2A, compare lanes 8 and 9), as expected on the basis of the slow rate of mismatch extension.



In an identical experiment with pol II $\Delta$ 9 ECs, cleavage was slower ( $k_{\text{obs}} = 0.01 \text{ min}^{-1}$ ) and less efficient (only about 30% cleavable) (Figure 2 panel A, lanes 10–17, and panel B, closed circles). As with the pol II ECs, all of the cleaved complexes remained in functional ECs that could be quickly elongated to 20 nt by addition of ATP, GTP, and CTP (10  $\mu\text{M}$  each) (Figure 2A, compare lanes 17 and 18). The different responses of pol II and pol II $\Delta$ 9 ECs was not the result of differential binding of TFIIS to the two types of complexes. The concentration of TFIIS used (10  $\mu\text{M}$ ) is sufficient to saturate both pol II and pol II $\Delta$ 9 ( $K_d \approx 80 \text{ nM}$  for each<sup>43</sup>), and we confirmed that both the rate and the extent of cleavage were the same at TFIIS concentrations between 7 and 30  $\mu\text{M}$  (data not shown).

These results demonstrate that Rpb9 affects transcriptional proofreading. The presence of Rpb9 slows extension of a mismatched 3' end, and the impact of slower mismatch extension is not nullified by a corresponding decrease in the rate of TFIIS-mediated cleavage. In fact, for the sequence context used in Figures 1B and 2, Rpb9 increases both the rate and efficiency of cleavage. In addition, our results are consistent with the idea that, at least in this sequence context, EC assembly with a mismatched 3' end generates two classes of complexes that do not rapidly interconvert, one class that can be efficiently elongated (favored when Rpb9 is absent), and another that can be efficiently cleaved (favored when Rpb9 is present). This is most directly seen in Figure 2A, lane 19, where complexes that are not cleavable can be elongated in the presence of the next correct NTP. The RNA products longer than 12 nt are likely the result of misincorporations and/or possible contamination of ATP with small amounts of GTP.

Interestingly, during preliminary experiments with 3'-end-mismatched ECs in which pol II was immobilized from whole cell extracts (WCE), we noticed a significant amount of RNA cleavage (generating a 9 nt RNA) during the assembly of the ECs, the extent of which correlated with the time taken for the preparation. To examine this in more detail, we prepared ECs as quickly as possible (Figure 3A, lane 1) and then followed the time course of the cleavage reaction, which proceeded with a rate ( $k_{\text{obs}} = 0.048 \text{ min}^{-1}$ ) and extent (75% cleavable, including those that had been cleaved before time 0) similar to that seen with TFIIS in the purified system (Figure 3 panel A, lanes 2–6, and panel B, open circles). As with the purified system, the cleaved RNAs remained in active ECs; addition of ATP, CTP, and GTP (10  $\mu\text{M}$  each) after 60 min resulted in rapid extension of the cleavage-generated 9-mer to longer RNAs up to 20 nt, whereas the small amount of 11-mer remaining (still containing the mismatch) was not efficiently extended during a 30 s incubation with NTPs (Figure 3A, compare lanes 6 and 7). To determine whether this cleavage activity was TFIIS-dependent, we assembled ECs with pol II immobilized from WCE derived from an otherwise isogenic *dst1* $\Delta$  strain. These ECs carried out RNA extension as efficiently as those derived from WCE of *DST1* cells or assembled with purified pol II, but in the absence of *DST1*-encoded TFIIS no cleavage activity was observed (data not shown). These results strongly suggest that the cleavage activity is mediated by TFIIS and that TFIIS stably and near stoichiometrically associates with pol II in the absence of an EC even after the extensive washes used in our immobilization protocol.

Pol II immobilized from a WCE prepared from an *rpb9* $\Delta$  strain also yielded results similar to those obtained with the purified system (Figure 3 panel A, lanes 8–13, and panel B,

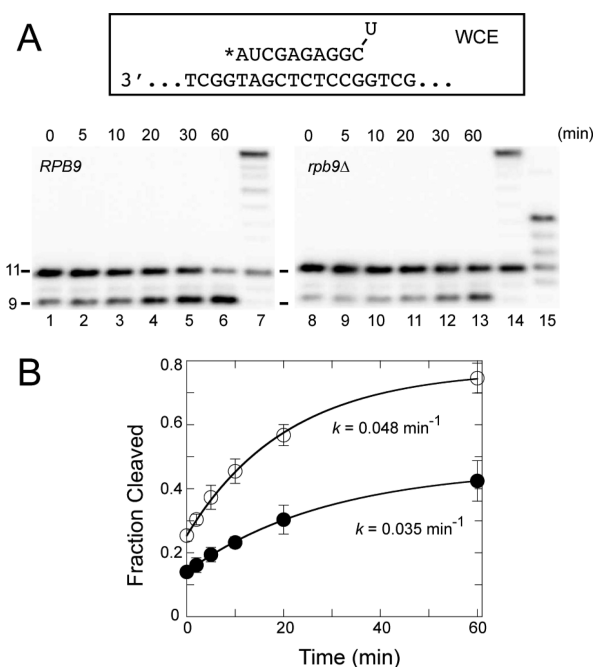


**Figure 3.** Cleavage of mismatched 3' ends by ECs assembled from WCE. (A) Time course of cleavage. ECs with a mismatched 3' end identical to that shown in Figure 1A were assembled using WCE derived from *RPB9* (lanes 1–7) or *rpb9* $\Delta$  (lanes 8–15) yeast. An abbreviated depiction of the EC is shown here for reference. These ECs were incubated in TB(40). Aliquots were removed at the indicated times, and the products were separated by denaturing polyacrylamide gel electrophoresis and visualized on a phosphorimager. After 60 min, ATP, CTP, and GTP (10  $\mu\text{M}$  each) were added to the reaction and incubated for 30 s (lanes 7 and 14). An aliquot of the ECs assembled with WCE derived from *rpb9* $\Delta$  cells was incubated for 60 min with ATP (250  $\mu\text{M}$ ) (lane 15). (C) Quantitation of the cleavage time course. The fraction of ECs cleaved to 9 nt was plotted against time and fit to a single exponential equation (open circles, *RPB9* WCE; closed circles, *rpb9* $\Delta$  WCE). Error bars indicate the SD for three independent experiments.

closed circles). As observed in experiments with purified components, ECs containing a 3' mismatch were less susceptible to cleavage than those with Rpb9 (approximately 40% cleavable, including those that had been cleaved before time 0), and all of the cleaved RNAs remained in functional ECs that could be quickly elongated to 20 nt by addition of ATP, GTP, and CTP (10  $\mu\text{M}$  each) (Figure 3A, compare lanes 13 and 14). As with the purified system, cleavage-resistant complexes were largely elongation-competent, which was demonstrated by their ability to incorporate ATP, the next correct nucleotide (Figure 3A, lane 15). (As in Figure 2A, the RNAs larger than the expected 12 nt extension product were likely the result of misincorporation and/or small amounts of GTP contamination.) Approximately 40% of the WCE-derived pol II $\Delta$ 9 ECs had been cleaved at the reaction end point, suggesting that TFIIS is associated with at least 40% of these complexes. However, because this fraction is very similar to the fraction of cleavable complexes formed when purified TFIIS is present in excess (Figure 2) and because Rpb9 apparently has no effect on binding of TFIIS to pol II,<sup>43</sup> TFIIS may actually be present in most, if not all, of the WCE-derived pol II $\Delta$ 9 ECs. One notable difference in our experiments with the purified and WCE systems is the faster rate of cleavage for pol II $\Delta$ 9 observed in the WCE system ( $k_{\text{obs}} = 0.035 \text{ min}^{-1}$ ). Although

this could be caused by unidentified WCE-derived proteins associated with the ECs, it might also be the result of native, intact TFIIS being present in the WCE system rather than the N-terminal-truncated TFIIS used in the purified system. However, there are no experimental conditions in which we have observed that the increased rate of mismatch extension by pol IIΔ9 is countered by an increased rate or efficiency of TFIIS-mediated mismatch cleavage, and thus the absence of Rpb9 compromises the ability of pol II to proofread transcription errors.

We considered the possibility that the effect of Rpb9 on the relative fractions of extendable and cleavable ECs containing a mismatched 3' end could be an artifact of assembling the EC with a preformed mismatch. To test this idea, we generated a G–U mismatch in situ by misincorporating UTP (1 mM) into a matched 3'-end EC, shown in Figure 4A, using pol II (lanes

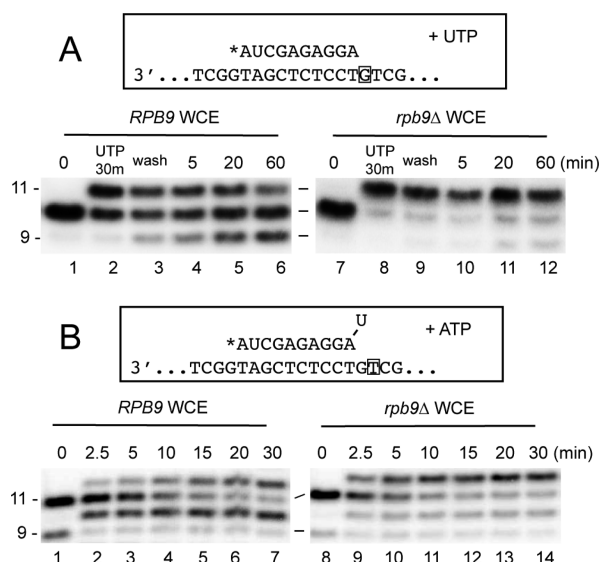


**Figure 4.** (A) Cleavage of in situ generated 3'-end mismatches. ECs with a matched 3' end were assembled using WCE derived from *RBP9* (lanes 1–6) or *rpb9Δ* (lanes 7–12) yeast. These ECs were identical to that shown in Figure 1A except as depicted (and with complementary template and nontemplate strands). The ECs were incubated with UTP (1 mM) to generate a mismatched 3' end (lanes 2 and 8), washed extensively to remove UTP (lanes 3 and 9), and then incubated in TB(40). Aliquots were removed at the indicated times (lanes 4–6 and 10–12), and the samples were separated by denaturing polyacrylamide gel electrophoresis and visualized on a phosphor-imager. (B) Effect of Rpb9 on proofreading a 3'-end mismatch. ECs with a mismatched 3' end were assembled with WCE derived from *RBP9* (lanes 1–7) or *rpb9Δ* (lanes 8–14) yeast. These ECs were identical to that shown in Figure 1A except as depicted (and with complementary template and nontemplate strands). The ECs were incubated with ATP (250 μM). Aliquots were removed at the indicated times, and the products were fractionated by denaturing polyacrylamide gel electrophoresis and visualized on a phosphor-imager.

1–6) or pol IIΔ9 (lanes 7–12) immobilized from WCE. We verified that the 3' ends of the extended complexes actually contained the mismatch by demonstrating that, unlike complexes with a matched end, they could not be rapidly extended by addition of NTPs (data not shown). This is not a trivial point, as some lots of NTPs are sufficiently contaminated that apparent misincorporation is actually caused by very low concentrations of contaminating correct nucleotide. The ECs

were extensively washed to remove UTP and then followed over time to assess cleavage. Similar to the results with ECs assembled with the mismatched end (Figures 2 and 3), the in situ generated mismatch was much more efficiently cleaved when Rpb9 was present (Figure 4A, compare lanes 3–6 and 9–12). Note that the sequence context for the G–U mismatch is slightly different from that used in Figure 2, suggesting that, although we have not checked a large variety of sequence contexts, the differential susceptibility to cleavage of pol II and pol IIΔ9 ECs is not limited to a specific context.

In a slightly different approach to assess the ability of Rpb9 to affect transcriptional proofreading, we assembled ECs with a mismatched 3' end and then added ATP (the next correct nucleotide) (Figure 4B), setting up conditions where both RNA extension and cleavage are possible. In this sequence context, cleavage of two nucleotides from the mismatched end generates a 9 nt product that can be rapidly extended by ATP, which is observed in the efficient extension of the 9 nt cleavage product generated during EC assembly (and present at time 0) to 10 nt during the first few minutes of the reaction (Figure 4B, compare lanes 1 and 8 with lanes 2 and 9). Thus, in this experiment, direct extension of the 11-nt-mismatched RNA generates a product of 12 nt, whereas cleavage of 2 nt generates a product of 10 nt after rapid extension of the resulting matched 9-mer by ATP. It is also possible that proofreading takes place after extension of the mismatch by cleavage of the extended 12-mer to 10 (see below). In either case, whether from cleavage of the mismatched 3' end (11 nt) or the extended mismatched 3' end (12 nt), the 10-mer represents a product derived from proofreading. Following the fate of the 11-mer present at time 0, over a period of 30 min approximately half was extended and half was cleaved using WCE containing pol II (Figure 4B, lanes 1–7), whereas for WCE containing pol IIΔ9, only about 10% was cleaved, with most of the remainder extended to 12 nt (lanes 8–14). This experiment strongly supports the conclusion that proofreading is much more efficient in the presence of Rpb9.

**Absence of Rpb9 Increases the Rate of Elongation beyond a Mismatched–Matched 3' End.** If a transcription error is not removed before the mismatched end is extended, then it is not clear at what point the mismatched base pair ceases to affect elongation or cleavage. To investigate this issue, we used purified pol II and pol IIΔ9 to assemble the EC shown in Figure 5A, which is designed to have a mismatch followed by a matched 3' end to simulate a situation in which a transcription error at position 11 has not been removed prior to addition of the next NTP. GTP was added, and the time course of extension from 12 to 13 nt was monitored (Figure 5). This experiment was performed at a low concentration of GTP to slow the reaction to a rate that could be easily measured. For pol II, the rate of mismatch–match extension ( $k_{\text{obs}} = 0.29 \text{ min}^{-1}$ ) was approximately 1 to 2 orders of magnitude slower than would be expected under these conditions for a completely matched EC based on a rate for the matched EC estimated from reported  $k_{\text{pol}}$  and  $K_{\text{M}}$  values.<sup>28</sup> Thus, this position provides a potential kinetic checkpoint subsequent to a transcription error that could be exploited in proofreading. The rate of mismatched–matched 3'-end extension for pol IIΔ9 ( $k_{\text{obs}} = 0.62 \text{ min}^{-1}$ ) was approximately 2-fold faster than that for pol II, indicating a role for Rpb9 in establishing this checkpoint. The fraction of ECs that could be extended did not depend in any significant way on Rpb9; for both pol II and pol IIΔ9, about 70% of the ECs could be extended with GTP. (Note that

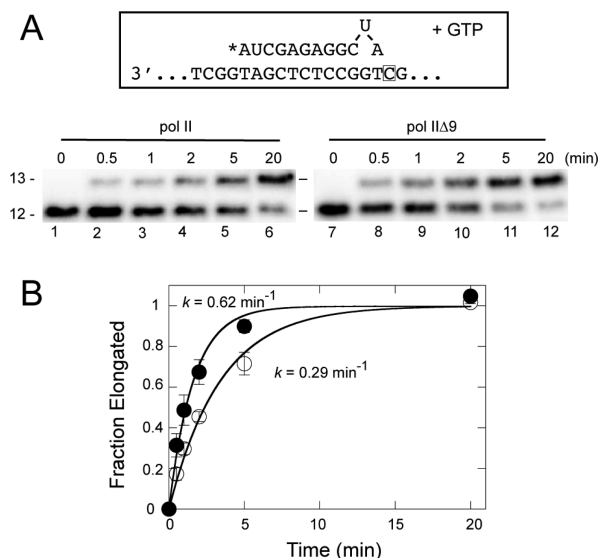


**Figure 5.** Effect of Rpb9 on extension of a mismatch-matched 3' end. (A) Time course of extension. ECs with a mismatch-matched 3' end were assembled with purified pol II (lanes 1–6) or pol IIΔ9 (lanes 7–12) and incubated with GTP (250  $\mu\text{M}$ ). These ECs were identical to that shown in Figure 1A except as depicted (and with complementary template and nontemplate strands). Aliquots were removed at the indicated times, and the products were separated by denaturing polyacrylamide gel electrophoresis and visualized on a phosphorimager. (B) Quantitation of the extension time course. The fraction of ECs extended to 13 nt was plotted versus time and fit to a single exponential equation (open circles, pol II; closed circles, pol IIΔ9). Error bars indicate the SD for three independent experiments. (Note that the y axis has been normalized to reflect only the ECs that are capable being elongated.).

the y axis in Figure 5B has been normalized to reflect only the ECs that are capable being elongated.)

**Rpb9 Promotes TFIIIS-Mediated Cleavage of a Mismatched-Matched 3' End.** To determine the potential for TFIIIS-mediated proofreading of a mismatched-matched 3' end, we exploited pol II and pol IIΔ9 immobilized from WCE, where we have shown that TFIIIS is stably associated with

essentially all pol II and a minimum of 40% of pol IIΔ9. Similar to our results with a mismatched 3' end (Figures 2 and 3), some of the mismatch-matched ends were cleaved during the assembly of the ECs using WCE with pol II. Interestingly, a 10-mer was the only significant cleavage product (Figure 6A, lane 1), indicating that the site of cleavage is between the mismatch and the nucleotide immediately preceding it. When GTP was added, ECs containing the mismatched-matched end were partitioned into two products, the cleaved 10-mer and a 13-mer resulting from extension with GTP (Figure 6A, lanes 1–10). Both of these products were within functional elongation complexes, as they could be rapidly extended by addition of ATP, GTP, and CTP (10  $\mu\text{M}$  each) (Figure 6A, lane 11). Taking into account only the 12-mer present at time 0, partitioning of the two products favored elongation by approximately 2 to 1, whereas the apparent rates of formation of the two products were essentially the same ( $k_{\text{obs}} \approx 0.3 \text{ min}^{-1}$ ) (Figure 6B). (Note that the y axis in Figure 6B reflects only the fate of the 12-mer that is present at time 0.) These observations are consistent with two possible interpretations: either the rates of extension and cleavage are fortuitously identical or there is a single population of pol II complexes containing the 12-mer that is subject to competing extension and cleavage reactions. In the latter case, partitioning of the two products would reflect the ratio of rate constants for the two reactions, whereas the identical observed rates would reflect their sum, giving estimates for the observed rate constants  $k_{\text{extension}}$  and  $k_{\text{cleavage}}$  of approximately  $0.2 \text{ min}^{-1}$  and  $0.1 \text{ min}^{-1}$ , respectively.

ECs with the mismatched-matched end behaved quite differently with WCE-derived pol IIΔ9. We observed essentially no cleavage, and the only product was the 13-mer generated by extension with GTP (Figure 6A, lanes 12–21). In addition, the rate of extension ( $k_{\text{obs}} = 0.41 \text{ min}^{-1}$ ) (Figure 6B) was about twice that estimated for pol II, consistent with the faster extension rate observed with the purified polymerases (Figure 5). These results indicate that in the absence of Rpb9, pol II is less able to take advantage of a potential proofreading checkpoint one nucleotide past a misincorporation event.

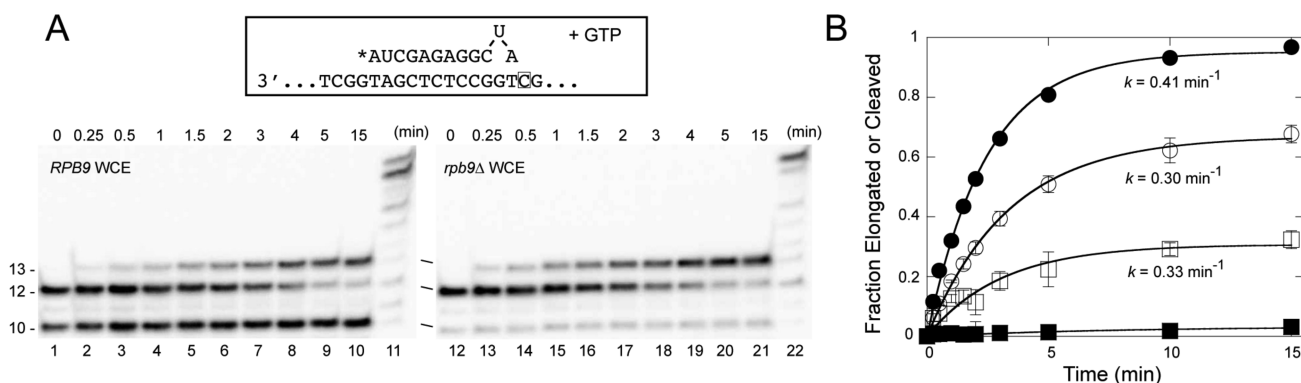


**Figure 6.** Effect of Rpb9 on proofreading a mismatch-matched 3' end. (A) ECs with a mismatch-matched 3' end were assembled with WCE derived from RPB9 (lanes 1–11) or *rpb9Δ* (lanes 12–22) yeast. These ECs were identical to that shown in Figure 1A except as depicted (and with complementary template and nontemplate strands). The ECs were incubated with GTP (1  $\mu\text{M}$ ). Aliquots were removed at the indicated times, and the products were separated by denaturing polyacrylamide gel electrophoresis and visualized with a phosphorimager. After 15 min, ATP and CTP (10  $\mu\text{M}$  each) were added to the reaction and incubated for 30 s (lanes 11 and 22). (B) Quantitation of the time course. The graph follows the extension or cleavage of ECs that contained a 12 nt RNA at time 0. ECs cleaved to 10 nt prior to time 0 are not included. Curves were derived from fits to a single exponential equation (open circles, RPB9 WCE extension; open squares, RPB9 WCE cleavage; closed circles, *rpb9Δ* WCE extension; closed squares, *rpb9Δ* WCE cleavage). Error bars indicate the SD for three independent experiments.



We also tested ECs with a mismatch followed by two matched ribonucleotides at its 3' end. Neither pol II nor pol II $\Delta$ 9 cleaved this RNA in the presence of TFIIS, and the extension kinetics were indistinguishable from those expected for a completely matched RNA using the assays available to us (data not shown). Thus, it appears that misincorporation slows elongation and provides an opportunity for proofreading for only one nucleotide past the position at which the error was made.

Overall, our results strongly support a role for Rpb9 in transcriptional proofreading. In the absence of Rpb9, mismatched or mismatched–matched 3' ends are 2- to 3-fold more rapidly extended, thus providing less time for removal of a transcription error. This more rapid rate of extension is not offset by a more rapid rate of error removal, and, at least in some sequence contexts, the efficiency of cleavage is markedly decreased in the absence of Rpb9.

**Rpb9 and NTP Selectivity.** Although we have examined the effects of Rpb9 on proofreading in a number of different sequence contexts, the effect of Rpb9 on selectivity has been tested in only a single context, a UTP-for-CTP misincorporation.<sup>28</sup> To extend these selectivity studies, we assembled ECs containing a RNA with a matched 3' end using purified pol II or pol II $\Delta$ 9, and ATP was added rather than the correct, template-specified CTP (Figure 7A). About 90% of the ECs could be extended to 11 nt under these conditions, but it was critical to show that the extended 3' end of the transcript actually contains a mismatch and was not the result of small amounts of contaminating CTP complementary to the template. In some cases, it has been possible to distinguish a mismatched 3' end by exploiting electrophoretic mobility differences between the matched and mismatched RNA products.<sup>28,40</sup> However, we have taken an approach that exploits the kinetic differences in pol II-mediated extension of matched and mismatched 3' ends. As shown in Figure 1, the rate of correct nucleotide extension from a mismatched 3' end is very slow, several orders of magnitude slower than from a matched end.<sup>4</sup> Consequently, a misincorporation would be expected to generate a product that would not be quickly extended after addition of other NTPs. A low concentration of ATP, CTP, and GTP (10  $\mu$ M) was added to duplicate samples representing the 90 min time points of the ATP misincorporation assays and then stopped after 30 s (Figure 7A, lanes 7 and 15); in each case, little if any of the 11-mer was extended by addition of these nucleotides, as would be expected for a mismatched 3' end. However, under these same conditions, the 10-mer with a matched 3' end (comparable to the 0 time point) was efficiently extended up to 20 nt (Figure 7A, lanes 8 and 16). The behavior of matched and mismatched 3' ends is best seen by comparing lanes 6 and 7 (Figure 7A), where upon the addition of NTPs most of the small amount of 10-mer remaining after the 90 min incubation with ATP was rapidly extended up to 20 nt, whereas the 11-mer was not significantly extended. These results provide strong evidence that essentially all of the 11-mer contains a mismatched 3' end.

The fraction of ECs extended to 11 nt was plotted versus time, and the data were fit to a single exponential equation to obtain  $k_{\text{obs}}$ . This experiment was repeated at a number of ATP concentrations, and the plot of  $k_{\text{obs}}$  versus [ATP] (Figure 7B) allowed us to determine  $K_M$  and  $k_{\text{pol}}$  for both pol II and pol II $\Delta$ 9 (Table 1).

NTP selectivity can be determined by comparing the catalytic efficiencies ( $k_{\text{pol}}/K_M$ ) for two different NTP substrates.

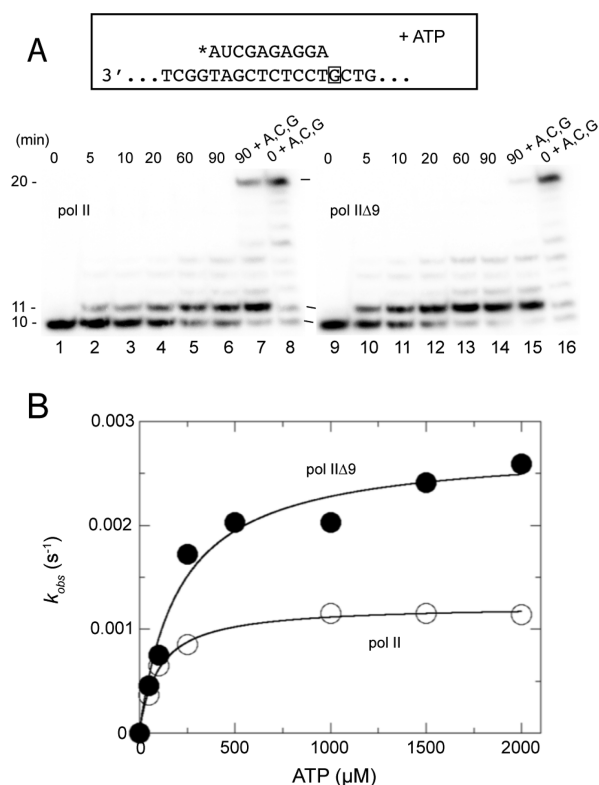


**Figure 7.** Effect of Rpb9 on ATP-for-CTP misincorporation. (A) ATP misincorporation time course. ECs with a matched 3' end were assembled with purified pol II (lanes 1–8) or pol II $\Delta$ 9 (lanes 9–16) and incubated with ATP (1 mM). These ECs were identical to that shown in Figure 1A except as depicted (and with complementary template and nontemplate strands). Aliquots were removed at the indicated times, and the products were separated by denaturing polyacrylamide gel electrophoresis and visualized with a phosphorimager. In lanes 7 and 15, samples identical to those in lanes 6 and 14, respectively, were incubated for an additional 30 s after addition of ATP, CTP, and GTP (10  $\mu$ M each). In lanes 8 and 16, samples identical to those in lanes 1 and 9, respectively, were incubated at room temperature for 90 min in the absence of NTPs and then for 30 s after addition of ATP, CTP, and GTP (10  $\mu$ M each). (B) Dependence of the misincorporation rate on [ATP]. Time-course experiments analogous to that shown in panel A were performed at several ATP concentrations, and the fraction of ECs extended to 11 nt was plotted versus time and fit to a single exponential equation. The  $k_{\text{obs}}$  at each concentration was plotted versus [ATP] (open circles, pol II; closed circles, pol II $\Delta$ 9), and the curves were obtained by fit to the Michaelis–Menten equation.

Although these values were easily measurable for the slow ATP misincorporation, determining the much faster rate of correct CTP incorporation requires quench-flow instruments that can measure times on the millisecond scale. However, at substrate concentrations well below  $K_M$ , the Michaelis–Menten equation reduces to a form in which a plot of  $k_{\text{obs}}$  versus substrate concentration yields a straight line with slope  $k_{\text{pol}}/K_M$ . Using CTP concentrations at or below 100 nM, where the rates are sufficiently slow to be measured without special instrumentation,  $k_{\text{pol}}/K_M$  for correct CTP addition for both pol II and pol II $\Delta$ 9 could be measured directly with the same ECs used to measure ATP misincorporation (Figure 8 and Table 1). For both pol II and pol II $\Delta$ 9, the NTP selectivity for correct CTP versus incorrect ATP was about  $3 \times 10^4$ , with no significant difference caused by the absence of Rpb9 (Table 1).

**Table 1. Effect of Rpb9 on ATP-for-CTP Selectivity<sup>a</sup>**

	NTP	$k_{\text{pol}}$ ( $\text{s}^{-1}$ )	$K_M$ ( $\mu\text{M}$ )	$k_{\text{pol}}/K_M$ ( $\text{s}^{-1} \mu\text{M}^{-1}$ )	selectivity
pol II	CTP (correct)			$0.31 \pm 0.01$	
	ATP (incorrect)	$(1.2 \pm 0.1) \times 10^{-3}$	$102 \pm 9$	$(1.2 \pm 0.2) \times 10^{-5}$	$(2.7 \pm 0.5) \times 10^4$
pol II $\Delta$ 9	CTP (correct)			$0.41 \pm 0.01$	
	ATP (incorrect)	$(2.7 \pm 0.1) \times 10^{-3}$	$206 \pm 43$	$(1.4 \pm 0.4) \times 10^{-5}$	$(3.2 \pm 1.0) \times 10^4$

<sup>a</sup>Kinetic parameters for ATP and CTP were derived from Figures 7B and 8, respectively.

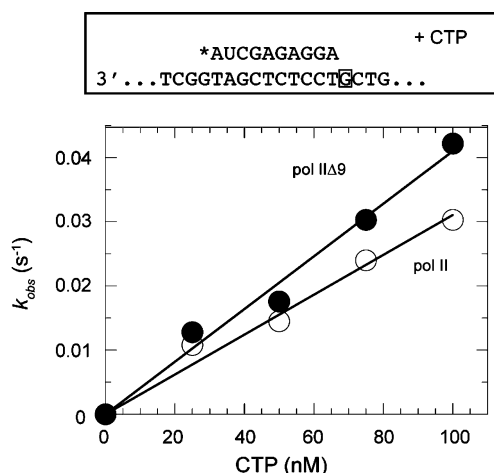


**Figure 8.** Catalytic efficiency for correct CTP addition. ECs were assembled with purified pol II or pol II $\Delta$ 9. These ECs were identical to that shown in Figure 1A except as depicted (and with complementary template and nontemplate strands). The time course of extension was measured at four different concentrations of CTP, and  $k_{\text{obs}}$  at each concentration was determined by a fit to a single exponential equation. The slope of the plot of  $k_{\text{obs}}$  vs [CTP] gives  $k_{\text{pol}}/K_M$  (open circles, pol II; closed circles, pol II $\Delta$ 9).

Interestingly, these results differ from those reported for correct CTP versus incorrect UTP, where loss of Rbp9 decreased selectivity by about 5-fold.<sup>28</sup> We therefore decided to examine UTP-for-CTP selectivity, and we took advantage of a competition assay adapted from one developed to assess selectivity between rNTP and dNTP by *E. coli* RNA polymerase.<sup>44</sup> The experimental design is summarized in Figure 9A. ECs with a RNA 10 nt in length were incubated with 1 mM UTP and a low (0.5–16 nM) concentration of CTP. Elongation with either of these substrates generates a RNA of 11 nt. To distinguish 11-mers with matched (C) or mismatched (U) ends, a low concentration of GTP (1  $\mu\text{M}$ ), the NTP complementary to the template at position 12, was also included. The matched-end 11-mer should very quickly be elongated to 12, whereas the mismatched-end 11-mer should not. Thus, RNAs of 11 and 12 nt should be indicative of incorrect (UTP) and correct (CTP) incorporation at position 11, respectively. Control experiments confirmed these expectations. UTP alone or a combination of UTP and CTP generated an 11-mer (Figure 9B, lanes 5, 6, 17, and 18), but only the CTP–GTP combination (Figure 9B, lanes 4 and 16) and not the UTP–GTP combination (Figure 9B, lanes 3 and 15) led to efficient extension to 12 nt. (The small amount of 12-mer in lanes 3 and 15 could include some UTP misincorporation at the mismatched end of the 11-mer.) In addition, the low concentration of GTP alone was not incorporated as a mismatch under these conditions (Figure 9B, lanes 2 and 14). When all three NTPs were present, the amount of 12-mer (correct CTP incorporation) increased

relative to the 11-mer (incorrect UTP incorporation) as the concentration of CTP was increased (Figure 9B, lanes 7–12 and 19–24). The relative amounts of CTP and UTP utilization at position 11 were quantitated, and corrections were made for the small fraction of mismatched U that was extended to 12 nt (Figure 9B, lanes 3 and 15) and for the appearance of the 13-mer that was likely derived from UTP misincorporation on the matched 3' end of the 12-mer. The CTP/UTP utilization ratio, indicative of correct/incorrect incorporation, was nearly identical for pol II and pol II $\Delta$ 9 at each of the CTP concentrations used (Figure 9C). The small differences observed at 8 and 16 nM CTP are in the direction of increased selectivity for pol II $\Delta$ 9, and this experiment provided no evidence for any decrease in selectivity in the absence of Rbp9.

## DISCUSSION

A number of studies<sup>18,45,46</sup> have suggested a kinetic model for substrate selectivity and RNA proofreading by RNA polymerase (Figure 10). In this model,  $n - 1$  represents an elongation complex with nascent RNA  $n - 1$  nucleotides in length whose 3'-terminal bases are completely complementary to the template. Extension of this RNA can follow two alternative paths. In one path, template-specified (correct, matched) NTPs can be added to the growing chain to generate ECs with RNAs containing  $n$  and then  $n + 1$  nucleotides, resulting in accurate transcription of the genetic information in the DNA template. Alternatively, an incorrect (mismatched) NTP can be added to generate an EC with a RNA whose 3' end is not complementary to the template ( $n^*$ ). The partitioning of  $n - 1$  to products  $n$  and  $n^*$  reflects the selectivity component of fidelity. Once an error has been generated by formation of  $n^*$ , there are again two alternative paths, which reflect the proofreading component of fidelity. The RNA containing the mismatch can be extended to  $n^* + 1$ , propagating the error, or the mismatched NMP can be eliminated through cleavage of the RNA, which, in most cases, occurs between the  $n - 2$  and  $n - 1$  NMPs for a mismatch at  $n^*$ . Cleavage generates a new, template-matched 3' end at  $n - 2$ ,<sup>42</sup> which provides a substrate for restarting accurate transcription. We have demonstrated here that proofreading can also occur at position  $n^* + 1$ , resulting in cleavage to  $n - 1$ , and that if the error is propagated to  $n^* + 2$  it is unlikely to be removed from the transcript.

Rbp9 clearly affects transcriptional proofreading. In its absence, pol II $\Delta$ 9 supports a faster rate of mismatch extension, decreasing the checkpoint period during which proofreading can occur, and this faster extension is not offset by a faster rate of TFIIS-mediated error removal. In fact, error removal is slower in the absence of Rbp9, and, in at least some sequence contexts, the extent of cleavage is adversely affected as well, suggesting that Rbp9 can affect the efficiency with which ECs adopt a conformation favorable for TFIIS-mediated cleavage. Thus, Rbp9 can affect transcriptional proofreading in three ways: by decreasing the rate of error propagation, by increasing



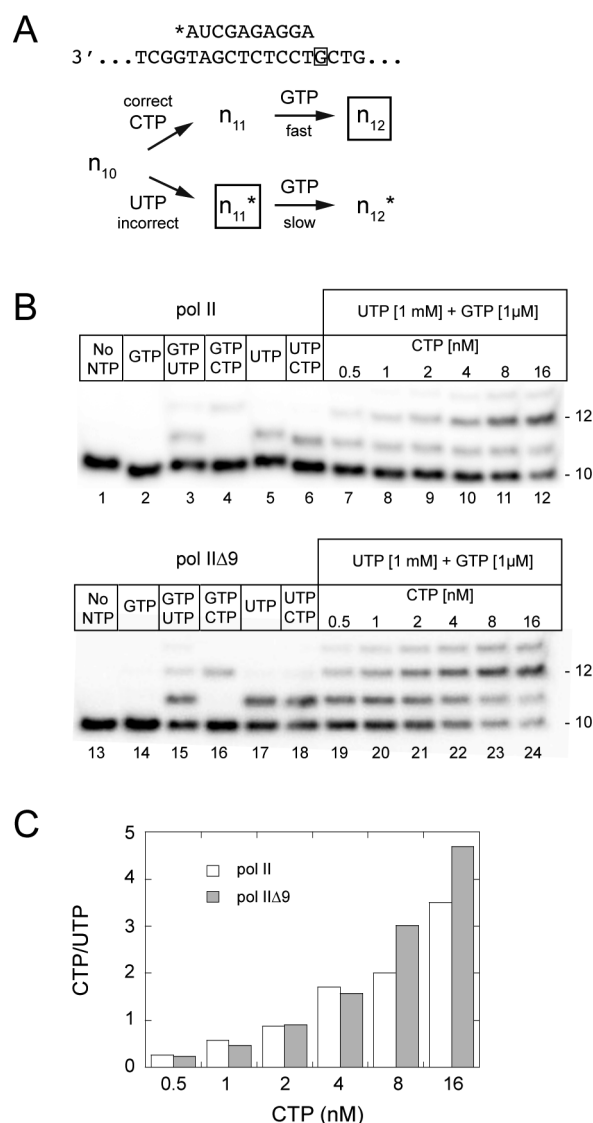


**Figure 9.** Effect of Rpb9 on UTP-for-CTP selectivity. (A) ECs were assembled with purified pol II or pol II $\Delta$ 9. These ECs were identical to that shown in Figure 1A except as depicted (and with complementary template and nontemplate strands). The diagram shows the expected outcomes for correct (CTP) or incorrect (UTP) extension in the presence of GTP (see text for details). (B) Pol II (lanes 1–12) and pol II $\Delta$ 9 (lanes 13–24) ECs were incubated for 10 min in the presence of no NTP substrate (lanes 1 and 13), GTP (1  $\mu$ M) (lanes 2 and 14), GTP (1  $\mu$ M) and UTP (1 mM) (lanes 3 and 15), GTP (1  $\mu$ M) and CTP (0.5 nM) (lanes 4 and 16), UTP (1 mM) (lanes 5 and 17), UTP (1 mM) and CTP (0.5 nM), or UTP (1 mM), GTP (1  $\mu$ M), and CTP (0.5–16 nM), as shown in the figure, lanes 7–12 and 19–24). The products were separated by denaturing polyacrylamide gel electrophoresis and visualized on a phosphor-imager. (C) Ratio of CTP incorporation to UTP incorporation at position 11 is shown for each of the CTP concentrations in panel B (lanes 7–12 and 19–24).

the rate of TFIIIS-mediated cleavage, and by favoring formation of an EC conformation in which cleavage is possible.

Our results can be interpreted in the context of X-ray crystal structures of ECs that contain RNAs with mismatched 3' ends. Two types of structures have been observed. In one type,<sup>12</sup> the polymerase is backtracked one nucleotide so that the last DNA–RNA base pair is at position +1, and the mismatched 3' end is in a novel location termed the P, or proofreading, site.

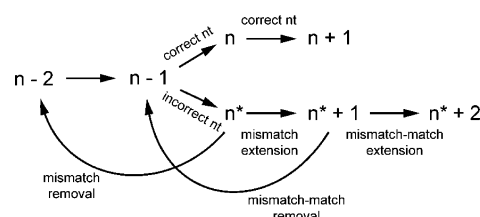


**Figure 10.** Model for transcriptional fidelity. See the text for details.

This conformation is likely similar to the substrate for TFIIIS-mediated cleavage between the –1 and +1 sites on the polymerase, resulting in the removal of 2 nt from the mismatched end of the RNA and generating a new matched 3' end ready for subsequent elongation. Our results are consistent with the idea that, at least in some sequence contexts, the presence of Rpb9 favors adoption of this backtracked, cleavage-competent conformation. In the second type of structure,<sup>40</sup> the polymerase is essentially in the post-translocated state, with the 3'-end mismatch at position –1 (present as a wobble base pair), and it is clearly not poised for cleavage. In addition, disruption and misalignment within the active site, including apparent loss of one of the catalytic metals, appears to preclude efficient extension of ECs in this conformation. It is possible that the absence of Rpb9 might favor a similar post-translocated conformation, consistent with the inefficient cleavage we observe. In addition, if the active-site disruptions seen in the crystal structure are in some way dependent on Rpb9, then this post-translocation positioning could explain the faster rate of mismatch extension observed with pol II $\Delta$ 9, where the disruptions may not occur.

If a mismatch is not removed before extension to  $n^* + 1$ , then further extension remains markedly slower than for an EC with RNA that is completely complementary to the template; this provides a second potential proofreading checkpoint. The mismatched–matched 3' end in such ECs is subject to TFIIIS-mediated cleavage, but further extension to  $n^* + 2$  precludes cleavage. Pol II $\Delta$ 9 supports a faster rate of mismatch–match extension, limiting the opportunity for error removal at this checkpoint. Furthermore, pol II $\Delta$ 9 mismatched–matched ECs are almost exclusively in a conformation that allows extension but limits cleavage. Rpb9 can thus affect proofreading at this checkpoint by decreasing error propagation and enhancing error removal.

Sydow et al.<sup>40</sup> have determined crystal structures of ECs containing mismatched–matched RNAs similar to those used in our study. In these structures, the mismatch (a wobble T–U base pair) is at position –1, and the 3' end, though complementary to the template, is in one of two “frayed” positions, one of which is similar to the P site described by Wang et al.<sup>12</sup> This structure has been described as a “paused, frayed” EC representing the first step in the process of backtracking and cleavage.<sup>47</sup> Our results are consistent with the idea that mismatched–matched pol II complexes can backtrack one step from this conformation to allow TFIIIS-mediated cleavage of 2 nt, whereas pol II $\Delta$ 9 complexes appear not to be able to efficiently backtrack and instead may favor the post-translocated state in which the next NTP can be added.

Walmacq et al.<sup>28</sup> have described a role for Rpb9 in maintaining the substrate selectivity of pol II. In their experiments, the absence of Rpb9 resulted in decreased discrimination by about 5-fold between correct (CTP) and incorrect (UTP) substrates. Our experiments did not detect a

significant effect of Rpb9 on selectivity in two sequence contexts, one of which was very similar to that in which the selectivity defect was previously observed. It is possible that the slight context difference in our work is the source of the different outcomes, which would suggest that selectivity is highly dependent on sequence context. However, selectivity is particularly difficult to measure when comparing two purine or two pyrimidine nucleotides. It is our experience that almost all commercial pyrimidine NTPs are contaminated with other pyrimidines, and purine NTPs are contaminated with other purines. This contamination is sufficient to interfere with experiments, as just a few parts per million contamination of the correct NTP is sufficient to compete with misincorporation. Of the many lots from many commercial suppliers we have tested, only one lot of UTP was sufficiently free of CTP to make the experiments in Figures 4 and 9 possible. Several aspects of the results of Walmacq et al. suggest that contamination may have been a problem in their experiments. First, the apparent rate of misincorporation did not approach saturation even at the highest concentrations of incorrect UTP tested (1500–2000  $\mu$ M), whereas the apparent first-order rate constants at these concentrations were several fold higher than we observe at saturation. In addition, the test for misincorporation presented, which was based on gel mobility differences of small RNAs with different 3' ends, was performed only at a relatively low concentration of UTP (100  $\mu$ M), leaving open the question of whether misincorporation remained the predominant reaction at higher concentrations of UTP.

Our results indicate that Rpb9 has multiple effects on transcriptional proofreading, but we were unable to observe an effect on substrate selectivity. After an error has been made, Rpb9 plays a role in slowing elongation to provide time for removal of the error, and it facilitates TFIIS-mediated RNA cleavage, at least in part, by facilitating efficient rearrangement of the EC into a conformation (presumably backtracked) necessary for cleavage. Rpb9 can affect proofreading at two checkpoints: either immediately after the error is introduced or after the error has been extended by addition of one nucleotide.

## AUTHOR INFORMATION

### Corresponding Author

\*E-mail: dopeterson@tamu.edu. Tel: 979-845-0953.

### Funding

This work was supported by NSF grant 0848085 to D.O.P.

### Notes

The authors declare no competing financial interest.

## ACKNOWLEDGMENTS

We thank Mikhail Kashlev for providing the yeast strain with affinity-tagged Rpb3; Craig Kaplan and Mary Bryk for sharing reagents, equipment, and advice; Diane Hawley for valuable discussions; and Adam Peterson and undergraduate students Jerrett Nunneley, Julianna Hudnall, and J. Colin Klingemann for technical assistance. The support of Texas A&M AgriLife Research is also gratefully acknowledged.

## ABBREVIATIONS USED

EC, elongation complex; NTP, nucleoside triphosphate; pol II, RNA polymerase II; pol II $\Delta$ 9, RNA polymerase II lacking the Rpb9 subunit; WCE, whole cell extract

## REFERENCES

- (1) de Mercoyrol, L., Corda, Y., Job, C., and Job, D. (1992) Accuracy of wheat-germ RNA polymerase II. General enzymatic properties and effect of template conformational transition from right-handed B-DNA to left-handed Z-DNA. *Eur. J. Biochem.* 206, 49–58.
- (2) Eire, D. A., Yager, T. D., and von Hippel, P. H. (1992) The single-nucleotide addition cycle in transcription: A biophysical and biochemical perspective. *Annu. Rev. Biophys. Biomol. Struct.* 21, 379–415.
- (3) Kaplan, C. D., Larsson, K. M., and Kornberg, R. D. (2008) The RNA polymerase II trigger loop functions in substrate selection and is directly targeted by alpha-amanitin. *Mol. Cell* 30, 547–556.
- (4) Kireeva, M. L., Nedialkov, Y. A., Cremona, G. H., Purtoy, Y. A., Lubkowska, L., Malagon, F., Burton, Z. F., Strathern, J. N., and Kashlev, M. (2008) Transient reversal of RNA polymerase II active site closing controls fidelity of transcription elongation. *Mol. Cell* 30, 557–566.
- (5) Wang, D., Bushnell, D. A., Westover, K. D., Kaplan, C. D., and Kornberg, R. D. (2006) Structural basis of transcription: Role of the trigger loop in substrate specificity and catalysis. *Cell* 127, 941–954.
- (6) Kaplan, C. D. (2013) Basic mechanisms of RNA polymerase II activity and alteration of gene expression in *Saccharomyces cerevisiae*. *Biochim. Biophys. Acta* 1829, 39–54.
- (7) Liu, X., Bushnell, D. A., and Kornberg, R. D. (2012) RNA polymerase II transcription: Structure and mechanism. *Biochim. Biophys. Acta* 1829, 2–8.
- (8) Martinez-Rucobo, F. W., and Cramer, P. (2012) Structural basis of transcription elongation. *Biochim. Biophys. Acta* 1829, 9–19.
- (9) Svetlov, V., and Nudler, E. (2012) Basic mechanism of transcription by RNA polymerase II. *Biochim. Biophys. Acta* 1829, 20–28.
- (10) Fish, R. N., and Kane, C. M. (2002) Promoting elongation with transcript cleavage stimulatory factors. *Biochim. Biophys. Acta* 1577, 287–307.
- (11) Kettenberger, H., Armache, K. J., and Cramer, P. (2004) Complete RNA polymerase II elongation complex structure and its interactions with NTP and TFIIS. *Mol. Cell* 16, 955–965.
- (12) Wang, D., Bushnell, D. A., Huang, X., Westover, K. D., Levitt, M., and Kornberg, R. D. (2009) Structural basis of transcription: Backtracked RNA polymerase II at 3.4 angstrom resolution. *Science* 324, 1203–1206.
- (13) Nesser, N. K., Peterson, D. O., and Hawley, D. K. (2006) RNA polymerase II subunit Rpb9 is important for transcriptional fidelity in vivo. *Proc. Natl. Acad. Sci. U.S.A.* 103, 3268–3273.
- (14) Shaw, R. J., Bonawitz, N. D., and Reines, D. (2002) Use of an in vivo reporter assay to test for transcriptional and translational fidelity in yeast. *J. Biol. Chem.* 277, 24420–24426.
- (15) Koyama, H., Ito, T., Nakanishi, T., Kawamura, N., and Sekimizu, K. (2003) Transcription elongation factor S-II maintains transcriptional fidelity and confers oxidative stress resistance. *Genes Cells* 8, 779–788.
- (16) Sigurdsson, S., Dirac-Svejstrup, A. B., and Svejstrup, J. Q. (2010) Evidence that transcript cleavage is essential for RNA polymerase II transcription and cell viability. *Mol. Cell* 38, 202–210.
- (17) Jeon, C., and Agarwal, K. (1996) Fidelity of RNA polymerase II transcription controlled by elongation factor TFIIS. *Proc. Natl. Acad. Sci. U.S.A.* 93, 13677–13682.
- (18) Thomas, M. J., Platas, A. A., and Hawley, D. K. (1998) Transcriptional fidelity and proofreading by RNA polymerase II. *Cell* 93, 627–637.
- (19) Acker, J., Wintzerith, M., Vigneron, M., and Keding, C. (1993) Structure of the gene encoding the 14.5 kDa subunit of human RNA polymerase II. *Nucleic Acids Res.* 21, 5345–5350.
- (20) Kaine, B. P., Mehr, I. J., and Woese, C. R. (1994) The sequence, and its evolutionary implications, of a *Thermococcus celer* protein associated with transcription. *Proc. Natl. Acad. Sci. U.S.A.* 91, 3854–3856.

- (21) Woychik, N. A., Lane, W. S., and Young, R. A. (1991) Yeast RNA polymerase II subunit RPB9 is essential for growth at temperature extremes. *J. Biol. Chem.* 266, 19053–19055.
- (22) Shcherbakova, P. V., Pavlov, Y. I., Chilkova, O., Rogozin, I. B., Johansson, E., and Kunkel, T. A. (2003) Unique error signature of the four-subunit yeast DNA polymerase epsilon. *J. Biol. Chem.* 278, 43770–43780.
- (23) Wery, M., Shematorova, E., Van Driessche, B., Vandenhaute, J., Thuriaux, P., and Van Mullem, V. (2004) Members of the SAGA and Mediator complexes are partners of the transcription elongation factor TFIIS. *EMBO J.* 23, 4232–4242.
- (24) Hull, M. W., McKune, K., and Woychik, N. A. (1995) RNA polymerase II subunit RPB9 is required for accurate start site selection. *Genes Dev.* 9, 481–490.
- (25) Jenks, M. H., O'Rourke, T. W., and Reines, D. (2008) Properties of an intergenic terminator and start site switch that regulate IMD2 transcription in yeast. *Mol. Cell. Biol.* 28, 3883–3893.
- (26) Furter-Graves, E. M., Hall, B. D., and Furter, R. (1994) Role of a small RNA pol II subunit in TATA to transcription start site spacing. *Nucleic Acids Res.* 22, 4932–4936.
- (27) Koyama, H., Ito, T., Nakanishi, T., and Sekimizu, K. (2007) Stimulation of RNA polymerase II transcript cleavage activity contributes to maintain transcriptional fidelity in yeast. *Genes Cells* 12, 547–559.
- (28) Walmacq, C., Kireeva, M. L., Irvin, J., Nedialkov, Y., Lubkowska, L., Malagon, F., Strathern, J. N., and Kashlev, M. (2009) Rpb9 subunit controls transcription fidelity by delaying NTP sequestration in RNA polymerase II. *J. Biol. Chem.* 284, 19601–19612.
- (29) Huang, Y., Intine, R. V., Mozlin, A., Hasson, S., and Maraia, R. J. (2005) Mutations in the RNA polymerase III subunit Rpc11p that decrease RNA 3' cleavage activity increase 3'-terminal oligo(U) length and La-dependent tRNA processing. *Mol. Cell. Biol.* 25, 621–636.
- (30) Chedin, S., Riva, M., Schultz, P., Sentenac, A., and Carles, C. (1998) The RNA cleavage activity of RNA polymerase III is mediated by an essential TFIIS-like subunit and is important for transcription termination. *Genes Dev.* 12, 3857–3871.
- (31) Kuhn, C. D., Geiger, S. R., Baumli, S., Gartmann, M., Gerber, J., Jennebach, S., Mielke, T., Tschochner, H., Beckmann, R., and Cramer, P. (2007) Functional architecture of RNA polymerase I. *Cell* 131, 1260–1272.
- (32) Lange, U., and Hausner, W. (2004) Transcriptional fidelity and proofreading in Archaea and implications for the mechanism of TFS-induced RNA cleavage. *Mol. Microbiol.* 52, 1133–1143.
- (33) Whitehall, S. K., Bardeleben, C., and Kassavetis, G. A. (1994) Hydrolytic cleavage of nascent RNA in RNA polymerase III ternary transcription complexes. *J. Biol. Chem.* 269, 2299–2306.
- (34) Chedin, S., Riva, M., Schultz, P., Sentenac, A., and Carles, C. (1998) The RNA cleavage activity of RNA polymerase III is mediated by an essential TFIIS-like subunit and is important for transcription termination. *Genes Dev.* 12, 3857–3871.
- (35) Ruan, W., Lehmann, E., Thomm, M., Kostrewa, D., and Cramer, P. (2011) Evolution of two modes of intrinsic RNA polymerase transcript cleavage. *J. Biol. Chem.* 286, 18701–18707.
- (36) Weilbaecher, R. G., Awrey, D. E., Edwards, A. M., and Kane, C. M. (2003) Intrinsic transcript cleavage in yeast RNA polymerase II elongation complexes. *J. Biol. Chem.* 278, 24189–24199.
- (37) Kireeva, M. L., Lubkowska, L., Komissarova, N., and Kashlev, M. (2003) Assays and affinity purification of biotinylated and non-biotinylated forms of double-tagged core RNA polymerase II from *Saccharomyces cerevisiae*. *Methods Enzymol.* 370, 138–155.
- (38) Baudin, A., Ozier-Kalogeropoulos, O., Denouel, A., Lacroute, F., and Cullin, C. (1993) A simple and efficient method for direct gene deletion in *Saccharomyces cerevisiae*. *Nucleic Acids Res.* 21, 3329–3330.
- (39) Brachmann, C. B., Davies, A., Cost, G. J., Caputo, E., Li, J., Hieter, P., and Boeke, J. D. (1998) Designer deletion strains derived from *Saccharomyces cerevisiae* S288C: A useful set of strains and plasmids for PCR-mediated gene disruption and other applications. *Yeast* 14, 115–132.
- (40) Sydow, J. F., Brueckner, F., Cheung, A. C., Damsma, G. E., Dengl, S., Lehmann, E., Vassilyev, D., and Cramer, P. (2009) Structural basis of transcription: Mismatch-specific fidelity mechanisms and paused RNA polymerase II with frayed RNA. *Mol. Cell* 34, 710–721.
- (41) Cipres-Palacin, G., and Kane, C. M. (1994) Cleavage of the nascent transcript induced by TFIIS is insufficient to promote read-through of intrinsic blocks to elongation by RNA polymerase II. *Proc. Natl. Acad. Sci. U.S.A.* 91, 8087–8091.
- (42) Izban, M. G., and Luse, D. S. (1993) SII-facilitated transcript cleavage in RNA polymerase II complexes stalled early after initiation occurs in primarily dinucleotide increments. *J. Biol. Chem.* 268, 12864–12873.
- (43) Awrey, D. E., Weilbaecher, R. G., Hemming, S. A., Orlicky, S. M., Kane, C. M., and Edwards, A. M. (1997) Transcription elongation through DNA arrest sites. A multistep process involving both RNA polymerase II subunit RPB9 and TFIIS. *J. Biol. Chem.* 272, 14747–14754.
- (44) Svetlov, V., Vassilyev, D. G., and Artsimovitch, I. (2004) Discrimination against deoxyribonucleotide substrates by bacterial RNA polymerase. *J. Biol. Chem.* 279, 38087–38090.
- (45) Alic, N., Ayoub, N., Landrieux, E., Favry, E., Baudouin-Cornu, P., Riva, M., and Carles, C. (2007) Selectivity and proofreading both contribute significantly to the fidelity of RNA polymerase III transcription. *Proc. Natl. Acad. Sci. U.S.A.* 104, 10400–10405.
- (46) Zenkin, N., Yuzenkova, Y., and Severinov, K. (2006) Transcript-assisted transcriptional proofreading. *Science* 313, 518–520.
- (47) Sydow, J. F., and Cramer, P. (2009) RNA polymerase fidelity and transcriptional proofreading. *Curr. Opin. Struct. Biol.* 19, 732–739.